

# Triclosan-loaded with high encapsulation efficiency into PLA nanoparticles coated with $\beta$ -cyclodextrin polymer

Amani El Fagui · Pierre Dubot · Thorsteinn Loftsson · Catherine Amiel

Received: 21 December 2011 / Accepted: 15 February 2012 / Published online: 9 March 2012  
© Springer Science+Business Media B.V. 2012

**Abstract** The purpose was to prepare triclosan-loaded polylactic acid nanoparticles containing  $\beta$ -cyclodextrin polymer shell, evaluate triclosan release from the particles using Franz diffusion cells and to study the stability of the particles in presence of a model protein, bovine serum albumin. The nanoparticles were prepared by a solvent displacement process. The nanoparticles were characterized by their size, encapsulation efficiency and morphology. They were of spherical shape with hydrodynamic diameter of about 100 or 200 nm depending on the polylactic acid used. Their high encapsulation efficiency ( $\sim 90\%$ ) indicated that triclosan is easily incorporated into the nanoparticles. The nanoparticles displayed slow and sustained triclosan release patterns (diffusion coefficient about  $10^{-22}$  m<sup>2</sup>/s) and the  $\beta$ -cyclodextrin polymer coating was stable under simulated physiological conditions. All these data indicated that these novel core-shell nanoparticles might provide a promising carrier system for controlled release of triclosan and other hydrophobic drugs after systemic administration.

**Keywords** PLA ·  $\beta$ -Cyclodextrin polymer · Nanoparticles · Triclosan · Bovine serum albumin

## Introduction

Controlled delivery of pharmacologically active agents from biodegradable nanoparticles (NPs) [1] has emerged as one of the eminent technological achievements during recent decades [2]. Synthetic polymers [3], such as poly(lactide acid) (PLA) and its copolymers poly(lactic acid-co-glycolid), have been widely used and reviewed due to their excellent biodegradability, biocompatibility and nontoxic properties. Also, surface modification or coating by hydrophilic polymers like polyethylene glycol [4] or polysaccharides [5] are known to protect NPs against uptake of the mononuclear phagocyte system (MPS) and enhance their stability [6]. The major challenges of development of NPs as delivery carriers are to control particle size and surface properties, to protect the encapsulated pharmaceutical agent and to deliver it in a controlled manner within the body [7, 8]. Very recently, we reported the design of novel PLA/ $\beta$ -cyclodextrin polymer (poly- $\beta$ -CD) NPs by direct adsorption of poly- $\beta$ -CD onto PLA NPs [9]. These systems have been fully characterized and the investigations showed that the poly- $\beta$ -CD is securely adsorbed to the NP surface and the shell thus formed can be viewed as a monolayer of poly- $\beta$ -CD coils. The shell, possessing  $\beta$ -CD units, is able to form non-covalent inclusion complexes with nonpolar compounds [10]. The purpose of the present investigation was to encapsulate triclosan (TCS) and evaluate its release behavior from the NPs in vitro using Franz diffusion cells. TCS is a hydrophobic antimicrobial agent [11] (Fig. 1). It was chosen as a model drug in this study due to its low aqueous solubility and ability of “host-guest” interaction with CDs. In addition, the stability of

A. El Fagui · C. Amiel (✉)  
Institut de Chimie et des Matériaux Paris Est, UMR 7182 CNRS,  
Université Paris Est, Equipe “Systèmes Polymères Complexes”,  
2-8 rue Henri Dunant, 94320 Thiais, Paris, France  
e-mail: amiel@icmpe.cnrs.fr

P. Dubot  
Institut de Chimie et des Matériaux Paris Est, UMR 7182 CNRS,  
Université Paris Est, Equipe “Métaux et Céramiques à  
Microstructures Contrôlées”, 2-8 rue Henri Dunant,  
94320 Thiais, Paris, France

T. Loftsson  
Faculty of Pharmaceutical Sciences, University of Iceland,  
Hofsvallagata 53, 107 Reykjavik, Iceland

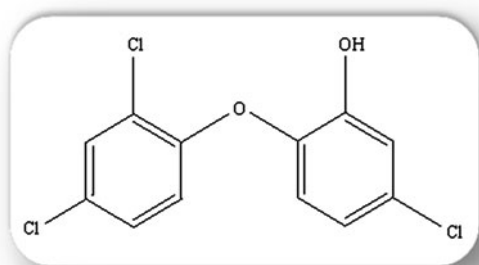


**Fig. 1** Structure of triclosan (2,4,4'-trichloro-2'-hydroxydiphenyl ether)

poly- $\beta$ -CD coated-PLA NPs in presence of a model protein, bovine serum albumin (BSA), was evaluated.

## Materials and methods

### Materials

The following chemicals were used as received: poly(D,L-lactic acid) (PLA-A and PLA-B, 50:50) polymers were purchased from (Phusis, Saint-Ismier, France), BSA was purchased from (Sigma-Aldrich, St. Louis, MO, USA), triclosan was donated by (Procter & Gamble, Egham, UK), (water solubility 10 mg/L at 25 °C), 2-hydroxypropyl- $\beta$ -cyclodextrin (HP- $\beta$ -CD) with molar substitution of 6 ( $M_w \sim 1,400$  g/mol) was purchased from (Roquette, Lestrem, France), acetone and methanol (HPLC Gradient Grade) were purchased from (VWR Fontenay sous Bois France). Ultrapurified water with Milli-Q Academic System, (Millipore, Billerica, MA, USA), was used throughout the study. Poly- $\beta$ -CD sample was prepared according to the procedure described previously [9]. Polymers characteristics are given in Table 1.

### Nanoparticles preparation

The TCS-loaded and unloaded PLA/poly- $\beta$ -CD NPs were prepared according to the nanoprecipitation method [5]. The typical procedure was as follows:

PLA-A or PLA-B (20 mg) with (or without) TCS (1 or 2 mg –10% or 20%–) were dissolved in acetone. The organic solution obtained was slowly added, drop by drop at room temperature, to 10 mL of the aqueous solution

without stabilizer under magnetic stirring. After adding all the organic phase to the aqueous phase, a homogeneous nanodispersion can be observed. Acetone was removed from the dispersion using rotating evaporator technique under reduced pressure. Then, a solution of poly- $\beta$ -CD containing 100 mg dissolved in 10 mL of water, prepared the day before in order to allow complete solubilization of the polymer, was added to the nanodispersion in an ice bath to avoid the rapid diffusion of the TCS in CDs cavities.

To remove the unadsorbed poly- $\beta$ -CD the NPs were ultracentrifuged (Beckman Coulter) at 40,000 rpm for 20 min at 4 °C.

Determination of loading capacity and encapsulation efficiency of the NPs

The amount of free TCS remaining in the supernatant was determined in the washing solutions after NPs ultracentrifugation by reverse phase high performance liquid chromatography (RP-HPLC) component system (Dionex Softron GmbH Ultimate 3000 Series, Germany), consisting of a P680 pump with a DG-1210 degasser, an ASI-100 autosampler, a VWD-3400 UV–vis detector operated at 283 nm and Phenomenex Luna C18 column (100 mm  $\times$  4.60 mm, 5  $\mu$ m). The mobile phase used consisted of water/methanol 10:90 (v/v) and the flow rate was 1.2 mL/min. The encapsulation efficiency (EE) was determined as the mass ratio of loaded TCS in NPs to the theoretical amount of TCS used for their preparation. The loaded TCS in NPs was expressed as loading capacity (LC) (mass ratio of loaded TCS to dry NPs).

### In vitro TCS release from core–shell NPs

The release behavior of TCS from PLA/Poly- $\beta$ -CD NPs was investigated in vitro using Franz diffusion Cells (FdC). The FdC (SES GmbH-Analysesysteme) consists of an upper donor chamber and a lower receiver compartment (Fig. 2). Donor and receptor compartments were separated by a semi-permeable cellophane membrane with a molecular cut off of 12–14 kDa (Spectrum Europe, Breda, The Netherlands). Before use, the membrane was soaked overnight in the receptor solution which had degassed under vacuum. The NPs used in release experiments had previously been lyophilized. Thus, after ultracentrifugation, the supernatants were removed and the pellets,

**Table 1** Polymer characteristics (see reference [9] for more details)

Sample	SEC/SLS		DSC $T_g$ (°C)	$^1\text{H NMR}$ % $\beta$ -CD (g/g)	DLS $R_H^a$ (nm)
	$M_w$ (g/mol)	$I_p$			
Poly- $\beta$ -CD	16,6000	1.4	–	51	5
PLA-A	35,400	1.3	53	–	Not soluble in water
PLA-B	79,700	1.8	55	–	

<sup>a</sup> Hydrodynamic radius in aqueous solution

reconstituted by mechanical agitation in an aqueous phosphate buffer solution (pH 7.4, 0.1 M) containing 2.5 or 5% HP- $\beta$ -CD, were freeze-dried after the freezing of the NPs suspension. 4.4 mg of NPs weighed and suspended in 2 mL of water were poured in the donor compartment of FdC, while the receptor compartment was filled with 12 mL of the same pH 7.4 phosphate buffer solution containing HP- $\beta$ -CD. The amount of HP- $\beta$ -CD needed to solubilize TCS was estimated from the determined phase-solubility diagrams of TCS in aqueous HP- $\beta$ -CD solutions (data not shown in this paper). The concentration of HP- $\beta$ -CD added to the receptor phase was chosen to ensure sink conditions during the experiment. The studies were conducted at room temperature ( $\sim 23$  °C) and at 37 °C under magnetic stirring of the receptor phase using a magnetic stirring bar (300 rpm). Samples of 150  $\mu$ L were removed from the receptor compartment at selected time intervals and replaced with an equal volume of fresh buffer. The concentration of TCS from the receptor phase was analyzed by the previously described RP-HPLC method.

#### Characterization of nanoparticles

##### *Nanoparticles size determination*

The size and size distribution of the uncoated and coated NPs were performed by dynamic light scattering (DLS). The hydrodynamic diameter ( $D_H$ ) and polydispersity index (PDI) were calculated using cumulant method. The thickness of the poly- $\beta$ -CD layer was calculated by subtracting the size of the uncoated NPs from the coated ones.

##### *Study of morphology of nanoparticles by scanning electron microscopy (SEM)*

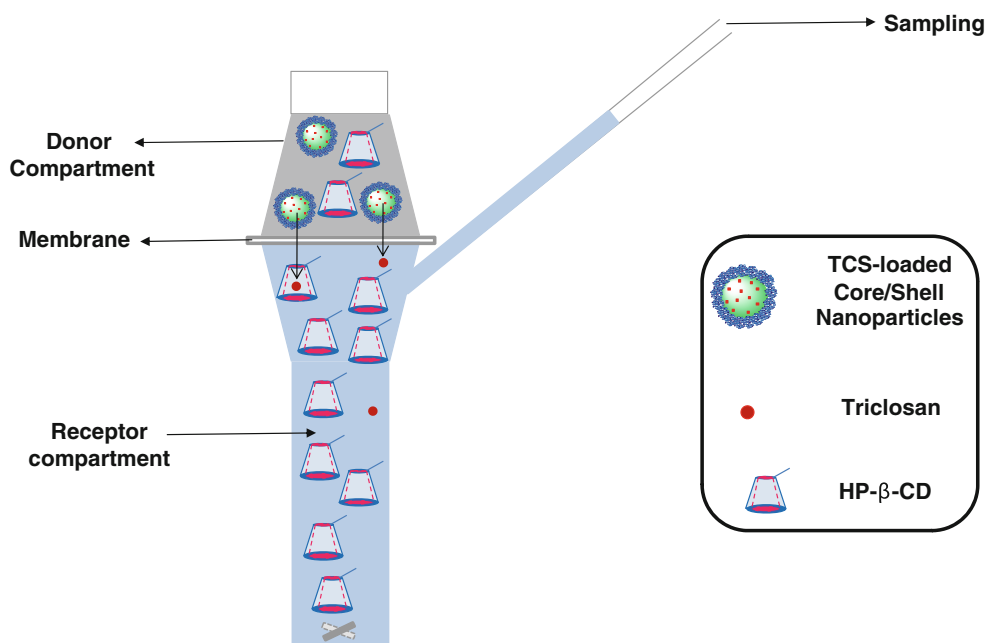
The morphological examination, such as shape and occurrence of aggregation phenomena, of NPs was performed by SEM using a scanning electron microscope (LEO 1530, LEO Microscopie Electronique France) equipped with a high-vacuum ( $10^{-10}$  mmHg) Gemini column and using InLens detector operated at an acceleration voltage of 1 kV. The NPs were deposited on mica surface and platinum/palladium coating was applied using sputter-coater (Cressington 208 HR) to make the NPs conductive. The samples were vacuum dried before examination.

##### *BSA adsorption study*

BSA adsorption study was carried out as described in the reference [12]. Briefly, 50 mg of freeze-dried unloaded NPs were put into contact with a BSA solution (0.7 mg/mL) and the adsorption was studied at 37 °C in phosphate buffer at pH 7.4 (0.05 M). After 24 h, the unadsorbed BSA was removed by ultracentrifugation. Then, the supernatant was collected and assayed spectrophotometrically (280 nm) to deduce the residual concentration of BSA (Cary 50, Varian Instruments).

The presence of BSA adsorbed at the NPs surface was also investigated using X-ray photoelectron spectroscopy (XPS). Particles were deposited onto a silicon wafer and introduced in an Ultra High Vacuum chamber with a residual pressure of  $3.0 \times 10^{-10}$  torr. XPS experiments were done with a MAC II Riber analyzer with an energy

**Fig. 2** Schematic representation of Franz diffusion cell used in the in vitro release experiments



resolution of 0.9 eV and a dual Mg–Al K $\alpha$  X-ray source used in a low power mode (11 keV, 5 mA) in order to minimize X-ray degradation. Survey scans were collected with 1.0 eV steps of 200 ms (30 scans) and photoelectrons take off angle was of 50°.

## Results and discussion

In our previous paper [9], novel PLA/poly- $\beta$ -CD NPs were successfully prepared by direct adsorption of poly- $\beta$ -CD onto preformed PLA NPs. The major goals of this study were to test the ability of the PLA(core)/poly- $\beta$ -CD(shell) NPs to load TCS and deliver it through a cellophane membrane using FdC, and to evaluate the stability of Poly- $\beta$ -CD coated-PLA NPs in presence of BSA. Unloaded and TCS-loaded core–shell NPs were successfully prepared by the solvent displacement method. PLA-A or PLA-B, differing by their molecular weights (see Table 1), were dissolved in acetone to form blank NPs. For loaded NPs, TCS was included in the process by dissolving it with PLA. The diameter of the unloaded PLA NPs was previously determined by DLS to be  $D_H$  (PLA-A) =  $82 \pm 2.0$  nm and  $D_H$  (PLA-B) =  $162 \pm 2.0$  nm [5].

### Physicochemical properties of core–shell NPs

The influence of TCS loading on NPs size was evaluated (Table 2). The results obtained for the coated and uncoated PLA-A and PLA-B NPs were then used to calculate the thickness of poly- $\beta$ -CD shell. The diameter of suspended NPs, as determined by DLS, varied from 87 to 202 nm with a very narrow PDI ( $\sim 0.1$  or less). Loading the NPs with TCS did not have any significant effect on their size.

The thicknesses of poly- $\beta$ -CD shells were about 20 nm except for PLA-B/poly- $\beta$ -CD/TCS 10% NPs where it was 30 nm. These values are greater than those obtained in our previous work of empty core–shell NPs (7–10 nm). It seems that the presence of TCS has an influence on the shell structure. It should be noticed that here the NPs were

redispersed in a pH 7.4 phosphate buffer solution containing HP- $\beta$ -CD. Thus, it is also possible that presence of HP- $\beta$ -CD influences the thickness of the poly- $\beta$ -CD shell.

As can be observed in Table 2, the EE and LC for TCS-loaded PLA/poly- $\beta$ -CD NPs were very high: EE between 60 and 88% (w/w) and LC between 11 and 32% (w/w). These results can be attributed to the good miscibility of TCS and PLA.

Uncoated PLA NPs could not be redispersed in water after freeze drying whereas PLA-B(core)/poly- $\beta$ -CD(corona) NPs were easily redispersed in water. The hydrophilic Poly- $\beta$ -CD coating clearly enhances the redispersion properties. The influence of the freeze drying on the NPs structure was studied by SEM (Fig. 3). The freeze-dried NPs reconstituted in water were deposited on mica and dried at room temperature. The NPs were spherical in shape with main size distribution close to 100 nm. Individual spherical structures can easily be observed showing that the coated NPs did not aggregate.

### In vitro TCS release kinetics

Release studies were carried out under sink conditions to understand the TCS release pattern. FdC method was selected for this purpose: the donor compartment was separated from the receptor compartment by a semi-permeable membrane allowing TCS, but not the NPs, to permeate from one compartment to the other. TCS loaded in PLA-A/poly- $\beta$ -CD/TCS 10% NPs were reported in this work. As shown in Fig. 4, the release kinetics consists of an initial release phase (burst) that is followed by a progressive zero order release of TCS. Here, the initial release is less than 5% and it can be attributed to the release of drug located close to the surface of NPs. From Fig. 4, we can also see that in vitro release at 25 °C showed, as expected, a slower release than at 37 °C. The temperature enhanced slightly the release. Thus, after 7 days at 37 °C, 45% of TCS contained in core–shell NPs had been released whereas only 39% at 25 °C.

The diffusion coefficient  $D^*$  of TCS can be determined from the release kinetics data using a mathematical model

**Table 2** Physicochemical properties of TCS-loaded PLA(core) NPs (A) and TCS-loaded PLA(core)/poly- $\beta$ -CD(shell) NPs (B)

(A)	PLA(core) NP <sub>s</sub>			(B)	PLA(core)/poly- $\beta$ -CD(corona) NP <sub>s</sub>				
	Ratio of TCS to PLA (g/g) (%)	Diameter (nm)	PDI		Ratio of TCS to PLA (g/g) (%)	Diameter (nm)	PDI	Thickness of poly- $\beta$ -CD corona (nm)	EE <sup>a</sup> (%)
A	10	87 ± 1	0.12	10	123 ± 1	0.1	18 ± 2	60 ± 8	11 ± 1.5
	20	87 ± 1	–	20	129 ± 1	0.1	21 ± 2	88 ± 3	32 ± 1
B	10	163 ± 2	0.08	10	224 ± 2	0.19	30 ± 4	75 ± 1	14 ± 1
	20	174 ± 2	0.05	20	202 ± 2	0.13	14 ± 4	76 ± 3	28 ± 1

<sup>a</sup> EE encapsulation efficiency (mass ratio of encapsulated TCS in NPs to the theoretical amount of TCS used in their preparation)

<sup>b</sup> LC loading capacity (TCS encapsulated in NPs)

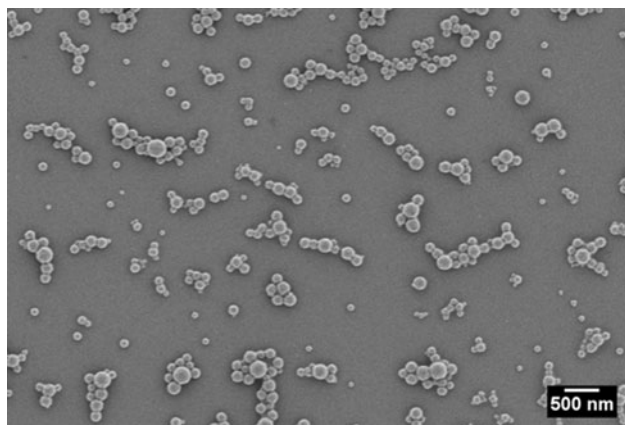


**Fig. 3** SEM image of freeze-dried unloaded PLA-B(core)/poly- $\beta$ -CD(corona)

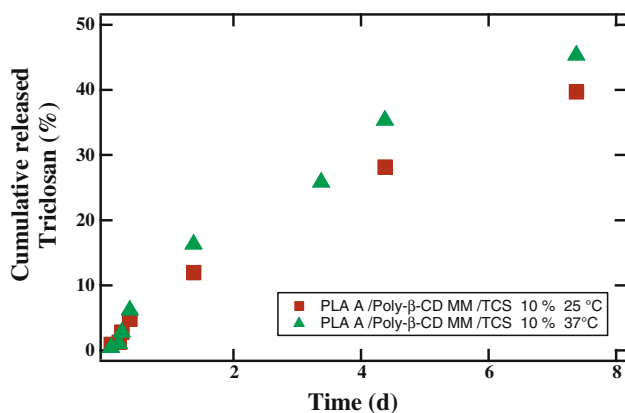


**Fig. 4** In vitro release profiles of TCS for BP-loaded PLA-A (core)/poly- $\beta$ -CD (corona) NPs. Ratios of PLA to TCS were 10% at 25 and 37 °C

derived from Fick's second law as TCS is molecularly dissolved into the NPs (data obtained by DSC not shown). Assuming spherical NPs the fraction of released TCS ( $M_t/M_\infty$ ) varies linearly with the square root of time at short times, as described [13]:

$$\frac{M_t}{M_\infty} = 6 \times \left( \frac{D^* t}{\pi R_s^2} \right)^{1/2} \quad (1)$$

$M_t/M_\infty$  is the fraction of TCS released at time  $t$ ,  $D^*$  is the diffusion coefficient of BP in the NPs and  $R_s$  is the radius of the spherical NPs.  $D^*$  can thus be calculated from the slope of  $M_t/M_\infty$  versus  $t^{1/2}$ .

Interestingly, very small  $D^*$  values ( $\sim 6 \times 10^{-22}$  m<sup>2</sup>/s) were obtained (Table 3). Other studies, where small molecules have been loaded in PLA NPs, gave  $D^*$  of about  $10^{-20}$  m<sup>2</sup>/s [12, 13].

The TCS release mechanism depends on two phenomena: first, a release from the PLA core to the poly- $\beta$ -CD

**Table 3** Modeling results of BP release

Ratio of TCS to PLA (g/g) (%)	Temperature of release medium (°C)	$D^*$ (m <sup>2</sup> /s)
10	25	$7.4 \times 10^{-22}$
	37	$5.9 \times 10^{-22}$

shell by diffusion and second, a release from the shell involving both diffusion and non-covalent guest–host interactions of TCS with CDs cavities present at the NPs surface. This explains partly the low diffusion coefficient obtained but does not account for the large difference with the literature values (i.e. they are more than 10 times lower). Another important aspect is the structural change of NPs that could be induced by freeze-drying. Indeed, in our previous work [9], the small angle neutron scattering study has revealed that without freeze drying, the PLA NPs contained traces of solvent in the center inducing a swollen core. The freeze-drying step could allow the elimination of the residual solvent and then the core becomes more rigid leading to a lag of release compared to NPs that have not been freeze-dried.

#### Stability of poly- $\beta$ -CD shell in presence of BSA

Human serum albumin is the most abundant protein in human blood plasma. When uncoated NPs are administered intravenously, they are rapidly opsonized and effectively cleared by the macrophages of MPS [6]. The size and surface of NPs determines the amount of blood components, mainly proteins, adsorbed to their surface. To reduce protein adsorption and prolong the circulation of NPs in vivo, the surface of our PLA NPs were coated with a hydrophilic shell based on poly- $\beta$ -CD. To study the stability of the coating, BSA was used as test protein. As described in the experimental part, the NPs were put into contact with a BSA solution. Uncoated PLA NPs were first studied as control. After 24 h contact between BSA and bare PLA NPs, the suspension was destabilized due to a strong interaction between BSA and PLA NPs surfaces. Under the same conditions, the core–shell NPs dispersion was still intact after 24 h of contact with BSA. After washing by ultracentrifugation-redispersion in water, the size of the NPs was analyzed by DLS. Its value, 209 nm, was slightly larger than the size of the unperturbed NPs (202 nm) indicating some BSA adsorption. Moreover, the supernatant was analyzed by UV and did not show any variation of the absorbance compared to the initial BSA solution. This result shows that the amount of BSA adsorbed was very small. The poly- $\beta$ -CD layer decreased the interactions of the NPs with BSA in comparison to uncoated PLA NPs.



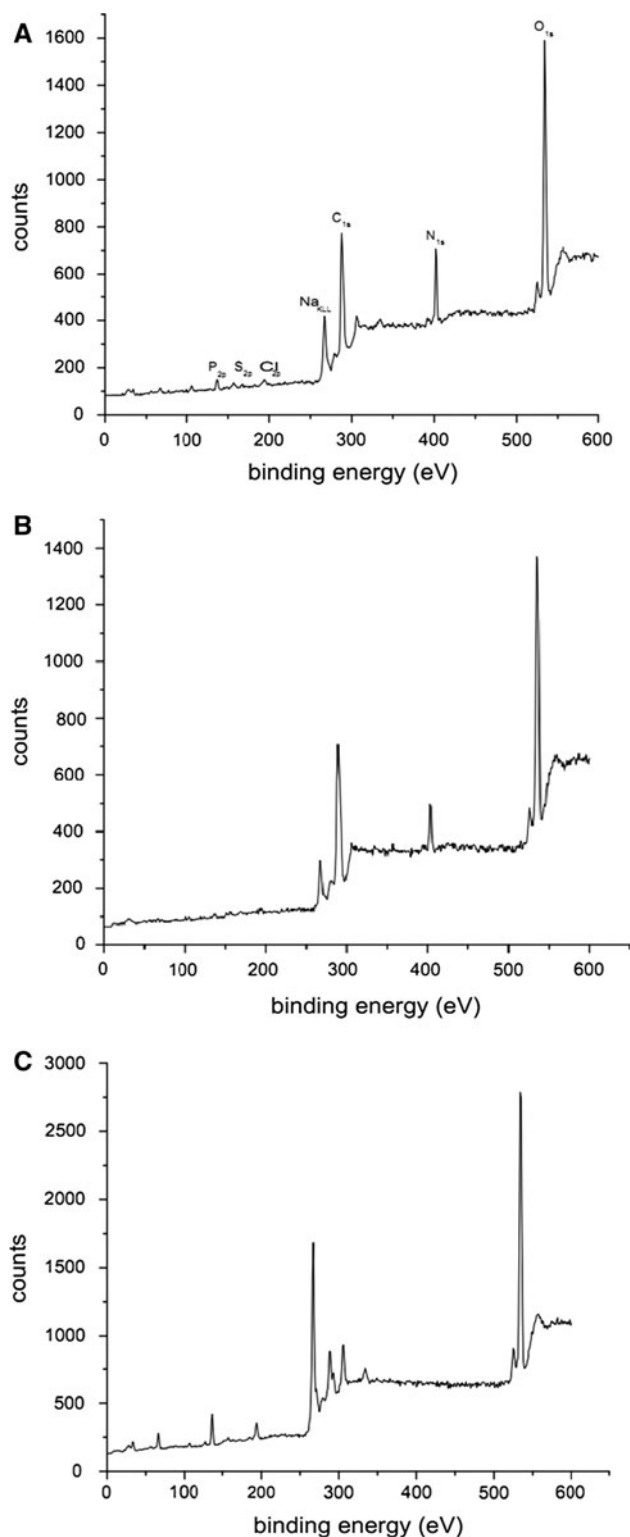


**Fig. 5** XPS spectra of BSA (a), poly- $\beta$ -CD/PLA NPs washed after incubation in BSA solution (b), blank poly- $\beta$ -CD/PLA NPs (c)

XPS technique, also known as ESCA (electron spectroscopy for chemical analysis), can reveal the elemental and chemical composition at the NPs' surface. It has thus

been chosen to confirm our previous result. Figure 5a shows the nitrogen ( $N_{1s}$ ) peak that is only present in BSA at 400.1 eV, corresponding to a binding energy of nitrogen of the amide group.  $C_{1s}$  peak is rather large (5 eV) and reveals three main components at 289 eV (carboxylate), 288 eV (amide bond) and 285 eV (C–H bond). The  $N_{1s}$  signal is absent from Fig. 5 (C) showing XPS spectra for poly- $\beta$ -CD/PLA NPs used as control but it is present in washed Poly- $\beta$ -CD/PLA NPs shown in Fig. 5b. We can notice the presence of Na  $KL_{23}L_{23}$  Auger main line appearing on the low binding energy side of the  $C_{1s}$  peak on Fig. 5a–c. We observed that the relative intensity of this line compared to  $C_{1s}$  or  $N_{1s}$  intensities strongly change from Fig. 5c to b. We believe that the important level of sodium concentration on the clean NP surface is due to the presence of ionized carboxylate on the NP surface (solution of pH near 7.0). The decrease of sodium concentration on the NP surface with adsorbed BSA (Fig. 5b), could be due to  $Na^+$  replacement by positively charged external BSA groups during the adsorption process. We can also remark, by comparing Fig. 5a and b, that the relative intensities of  $C_{1s}$  and  $N_{1s}$  do change during the adsorption process. This modification of the relative intensities can be due to BSA conformation change resulting from the interaction with the NP surface. It can also be inferred to the partial surface coverage of BSA. This last interpretation is in good agreement with the analysis of BSA concentration in supernatant.

These results proved that poly- $\beta$ -CD probably ensures inhomogeneous protection from BSA protein adsorption but it plays a predominant role. Indeed, without its presence PLA NPs cannot be resuspended after ultracentrifugation and after freeze-drying.

## Conclusion

This study shows the high encapsulation efficiency of TCS in PLA(core)/poly- $\beta$ -CD(shell) NPs. Loaded NPs could be freeze dried and resuspended in aqueous solution without morphological change as confirmed by SEM study. The NPs were spherical and DLS indicated that their size was about 100 or 200 nm depending on PLA used. TCS release profiles were characterized by a rapid initial release during the first couple of hours that was followed by a slow release phase. Under the assumption of a diffusion controlled mechanism, lower diffusion coefficient (around  $6 \times 10^{-22} \text{ m}^2/\text{s}$ ) were observed than previously reported for core-shell PLA NPs. Core-shell NPs studied in simulated physiological conditions were shown to possess good stability but residual BSA adsorption could be detected by XPS.

## References

1. Soppimath, K.S., Aminabhavi, T.M., Kulkarni, A.R., Rudzinski, W.E.: Biodegradable polymeric nanoparticles as drug delivery devices. *J. Control. Release* **70**(1–2), 1–20 (2001)
2. Uhrich, K.E., Cannizzaro, S.M., Langer, R.S., Shakesheff, K.M.: Polymeric systems for controlled drug release. *Chem. Rev.* **99**(11), 3181–3198 (1999)
3. Nair, L.S., Laurencin, C.T.: Biodegradable polymers as biomaterials. *Prog. Polym. Sci.* **32**(8–9), 762–798 (2007)
4. Marcato, P.D., Duran, N.: New aspects of nanopharmaceutical delivery systems. *J. Nanosci. Nanotechnol.* **8**(5), 2216–2229 (2008). doi:[10.1166/jnn.2008.274](https://doi.org/10.1166/jnn.2008.274)
5. Lemarchand, C., Gref, R., Couvreur, P.: Polysaccharide-decorated nanoparticles. *Eur. J. Pharm. Biopharm.* **58**(2), 327–341 (2004). doi:[10.1016/j.ejpb.2004.02.016](https://doi.org/10.1016/j.ejpb.2004.02.016)
6. Moghimi, S.M., Hunter, A.C., Murray, J.C.: Long-circulating and target-specific nanoparticles: theory to practice. *Pharmacol. Rev.* **53**(2), 283–318 (2001)
7. del Valle, E.M.M., Galan, M.A., Carbonell, R.G.: Drug delivery technologies: the way forward in the new decade. *Ind. Eng. Chem. Res.* **48**(5), 2475–2486 (2009). doi:[10.1021/ie800886m](https://doi.org/10.1021/ie800886m)
8. Mohamed, F., van der Walle, C.F.: Engineering biodegradable polyester particles with specific drug targeting and drug release properties. *J. Pharm. Sci.* **97**(1), 71–87 (2008). doi:[10.1002/jps.21082](https://doi.org/10.1002/jps.21082)
9. El Fagui, A., Dalmas, F., Lorthioir, C., Wintgens, V., Volet, G., Amiel, C.: Well-defined core-shell nanoparticles containing cyclodextrin in the shell: a comprehensive study. *Polymer* **52**(17), 3752–3761 (2011). doi:[10.1016/j.polymer.2011.06.043](https://doi.org/10.1016/j.polymer.2011.06.043)
10. Brewster, M.E., Loftsson, T.: Cyclodextrins as pharmaceutical solubilizers. *Adv. Drug Deliv. Rev.* **59**(7), 645–666 (2007). doi:[10.1016/j.addr.2007.05.012](https://doi.org/10.1016/j.addr.2007.05.012)
11. Loftsson, T., Leeves, N., Bjornsdottir, B., Duffy, L., Masson, N.: Effect of cyclodextrins and polymers on triclosan availability and substantivity in toothpastes in vivo. *J. Pharm. Sci.* **88**(12), 1254–1258 (1999)
12. Rouzes, C., Leonard, M., Durand, A., Dellacherie, E.: Influence of polymeric surfactants on the properties of drug-loaded PLA nanospheres. *Colloids Surf B Biointerfaces* **32**(2), 125–135 (2003). doi:[10.1016/s0927-7765\(03\)00152-8](https://doi.org/10.1016/s0927-7765(03)00152-8)
13. Romero-Cano, M.S., Vincent, B.: Controlled release of 4-nitro-anisole from poly(lactic acid) nanoparticles. *J. Control. Release* **82**(1), 127–135 (2002)